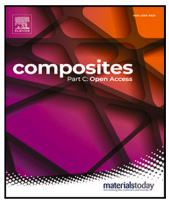
Composites Part C: Open Access 17 (2025) 100586



Contents lists available at ScienceDirect

Composites Part C: Open Access

journal homepage: www.elsevier.com/locate/composites-part-c-open-access





Correlating fluorescence and residual stiffness in self-reporting microcapsule composites with an intact soft matrix

David Schwarz [a], Viacheslav Slesarenko [a,b,*]

[a] Cluster of Excellence livMatS @ FIT – Freiburg Center for Interactive Materials and Bioinspired Technologies, University of Freiburg, Freiburg, 79110, Germany
[b] Department of Microsystems Engineering, University of Freiburg, Freiburg, 79110, Germany

ARTICLE INFO

MSC:
74E30
74A40

Keywords:
Self-reporting
Microcapsules
Composites
Damage
Soft materials
Stiffness

ABSTRACT

Self-reporting microcapsule-based systems are highly valuable for providing information about a composite's health, whether by indicating the location of damage or, in more advanced cases, reflecting the extent of damage through intensity of fluorescence. However, measuring such intensity alone is insufficient for evaluating the deterioration of a composite's mechanical properties. Using self-reporting stiff capsules containing tetraphenylethylene (TPE) and hexyl acetate embedded in a soft polymeric matrix, we observe that accurately assessing mechanical properties after damage in evaporation-based self-reporting systems requires not only measuring fluorescence brightness but also accounting for the time elapsed since the rupture of the capsules. While the fluorescence–stiffness correlation can be approximated by a linear fit at any given time, the proportionality coefficient gradually evolves, stabilizing only hours after capsule rupture. This study highlights the importance of considering the transient nature of fluorescence–stiffness relationships when leveraging self-reporting composites for advanced damage evaluation.

1. Introduction

Combining multiple materials into a single composite often pursues the aim of enhancing overall mechanical properties, such as stiffness or toughness [1]. However, it is also possible to introduce additional functionalities via the composite structure. One such functionality is self-healing — the material's ability to repair itself — which is often achieved by incorporating vascular networks [2,3] or filled capsules within the matrix material [4–6]. In the latter approach, a propagating crack in the composite ruptures the capsules along its path, releasing a healing agent that reacts with catalysts embedded in the matrix [7,8]. This reaction leads to in-situ polymerization, effectively repairing the mechanically induced damage [9,10]. Extensive research has investigated various matrix and capsule combinations, demonstrating a wide range of mechanical properties and chemical mechanisms that enable self-healing functionality [11–15].

Any degree of damage, including regions that have been allegedly healed, often results in inferior mechanical properties compared to the composite's original, intact state [9,10,16]. Therefore, identifying such damaged regions, whether healed or not, is crucial. Similar to self-healing, self-reporting can be achieved by embedding dye-filled capsules within the matrix material [17–19]. Upon rupture, the release of the capsule's contents can activate chemical processes that visually distinguish damaged areas from undamaged ones [20–22]. Of particular interest are self-reporting capsules that indicate damage through color changes or fluorescence [17,21,23,24]. Depending on the design and the loading conditions, two main scenarios might take place. In the case when capsule rupture happens simultaneously with the occurrence of damage in the matrix, as in incisions [17], self-reporting informs directly about the damage in the matrix. However, the capsules can be ruptured even when the matrix is still intact due to achieving locally the critical stress level [25]. Here, the visual self-reporting just highlights the reaching of some specific strain or stress level and partially resembles self-sensing when the overall strain state is acquired [26]. For the design of composites containing capsules, special attention should be directed to the assessment of the capsule's contribution to the composite's mechanical properties. The shape [27] and size [28] of capsules play a significant role in the overall mechanical behavior of the composite before and after their rupture. Depending on the goals, capsules can be deliberately designed before incorporation, since the existing fabrication processes allow them to be manufactured down to the nanometer range [29,30]. If the matrix is not getting damaged while some capsules break, one might tune the contrast between the stiffness of intact and damaged composites.

The partial recovery of mechanical properties in self-healing microcapsule composites is relatively slow due to the time required for

* Corresponding author.
E-mail address: viacheslav.slesarenko@livmats.uni-freiburg.de (V. Slesarenko).

https://doi.org/10.1016/j.jcomc.2025.100586
Received 16 January 2025; Received in revised form 15 March 2025; Accepted 4 April 2025
Available online 18 April 2025
2666-6820/© 2025 The Authors. Published by Elsevier B.V. This is an open access article under the CC BY license (http://creativecommons.org/licenses/by/4.0/).

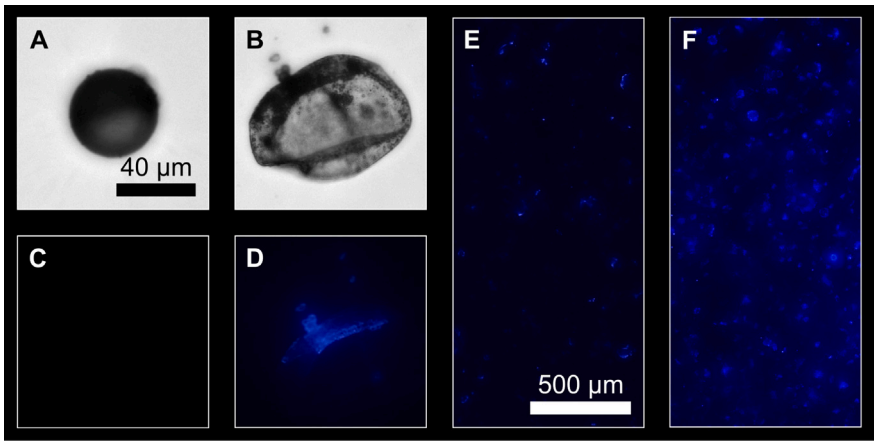


Fig. 1. (A, B): Micrograph of a single intact and ruptured microcapsule, respectively. (C, D): Fluorescence signal of a single intact and ruptured microcapsule, respectively. (E, F): Fluorescence of PDMS specimen with embedded microcapsules before (E) and after (F) rupture.

the chemical reactions involved in the healing process [10,31]. To prevent the use of materials after partial damage but before healing is complete, self-reporting systems are expected to respond more rapidly [32]. However, depending on the chemical mechanism underlying the reporting system, a delay between capsule rupture and damage detection may still occur, and this delay is particularly pronounced in evaporation-based fluorescent reporting systems [21,33,34]. Among the various mechanisms that rely on evaporation to trigger fluorescence, aggregation-induced emission (AIE) is one of the most commonly used for damage reporting. Initially, an AIE luminogen, such as tetraphenylethylene (TPE), is dispersed in a solvent and remains non-fluorescent. Upon rupture of the microcapsule containing the solution, the solvent evaporates, causing the luminogen to aggregate and fluoresce under UV light, thereby facilitating damage detection [21,35].

Notably, the intensity of the visual signal can be correlated to the extent of the damage or the number of ruptured capsules in the composite, as demonstrated in studies of localized impacts and incisions [21,34]. Given that fluorescence saturation may take hours, whereas the mechanical consequences of the capsules breaking are instantaneous [20], it raises the question of how reliably the extent of damage can be correlated with the fluorescence brightness at any given moment.

In this study, we address this using poly(dimethylsiloxane) (PDMS) with embedded poly(urea formaldehyde) (PUF) capsules. The widely used silicone-based elastomer PDMS, selected as a matrix material, exhibits excellent mechanical properties, including high elasticity and durability, while its relatively low viscosity facilitates easy molding and precise replication of fine structures [36]. Complementing other studies that focus on locally induced damage [10,12,17,25], here we subject the specimens to non-local tensile loading, causing capsule rupture throughout the entire volume of the specimen. This approach allows us to monitor the overall fluorescence brightness as well as mechanical properties over several hours following capsule rupture and correlate them to each other.

2. Materials and methods

Polyurethane/poly(urea-formaldehyde) (PU/UF)-based core–shell microcapsules containing a 1 wt% (8.7 $\mathrm{mg\,mL^{-1}}$, 26 mM) solution of TPE in hexyl acetate were prepared using a well-established single-batch in situ emulsification–condensation method, similar to that described in [21,33,37,38]. The capsules had a diameter of 41 ± 17 µm, similar to those used in the recently published work by Stamp et al. [39]. These microcapsules, containing the TPE/hexyl acetate solution, are colorless under visible light (Fig. 1A) and non-emissive under UV-A irradiation (λ = 365 nm) (Fig. 1C). When the microcapsule shells are ruptured by mechanical stress, the solution is released, leading to evaporation of the hexyl acetate (Fig. 1B). This evaporation causes the TPE to aggregate, emitting blue light under UV-A irradiation (Fig. 1D). After successfully fabricating the microcapsules, tensile specimens were prepared via molding. The specimens were produced by incorporating 10 wt% microcapsules into commercially available poly(dimethylsiloxane) (PDMS), Sylgard 184 (Dow, Midland, USA). The mixture was degassed, then poured into two-piece molds machined from poly(methyl methacrylate) (PMMA), and cured in an oven at 100 °C for 30 min. Each fabrication batch produced at least five specimens with dimensions closely resembling ISO 37 type 2, along with a reference disk-shaped specimen of 20 mm in diameter.

The PDMS-microcapsule composite with intact capsules initially exhibits negligible emission in the blue region of the visible spectrum (λ_{max} = 455 nm) under UV-A irradiation (λ = 365 nm) (Fig. 1E). When the shells of the microcapsules in the composite were ruptured by mechanical stress (e.g., stretching), fluorescence (λ_{max} = 455 nm) became observable (Fig. 1F). The intact specimens were then mechanically tested using a uniaxial testing machine (ZwickRoell, Ulm, Germany) equipped with a 500 N load cell (Fig. 2). To monitor changes in fluorescence, the specimens were continuously illuminated with UV-ring light (λ = 365–375 nm), and a video was recorded using a CMOS camera (IDS UI-3880CP, IDS Imaging Development Systems GmbH, Obersulm, Germany) synchronized with the testing machine. A reference disk (non-damaged) was included within the video frame, while the entire test setup was covered with light-tight fabric to minimize the influence of ambient light.

The mechanical testing procedure included two different types of loading, both conducted in displacement-controlled settings. During the so-called load cycle, the specimen was stretched to a predefined displacement, triggering the partial breaking of the embedded capsules, and then unloaded to zero force. While it is almost impossible to accurately count the number of broken capsules, their number positively correlates with the magnitude of the applied deformation. As will be shown later, larger applied deformation is associated with more pronounced changes in the composite's behavior. To evaluate Young's modulus, so-called probing cycles were used before (20 cycles) and after (880 cycles) the load cycle (Fig. 2B). Each probing cycle consisted of stretching up to 2 mm at a rate of 8 $\mathrm{mm\,min^{-1}}$, followed by unloading to zero force at the same rate and a subsequent hold time of 30 s. Preliminary tests indicated that such a small stretch does not cause capsule rupture but allows the assessment of Young's modulus from force–displacement data. Stress was calculated from the force by dividing it by the initial cross-section in the center of the specimen, while strain was obtained by referencing the initial length of the specimen (i.e., the distance between fixtures). A correction factor of 0.52, determined by

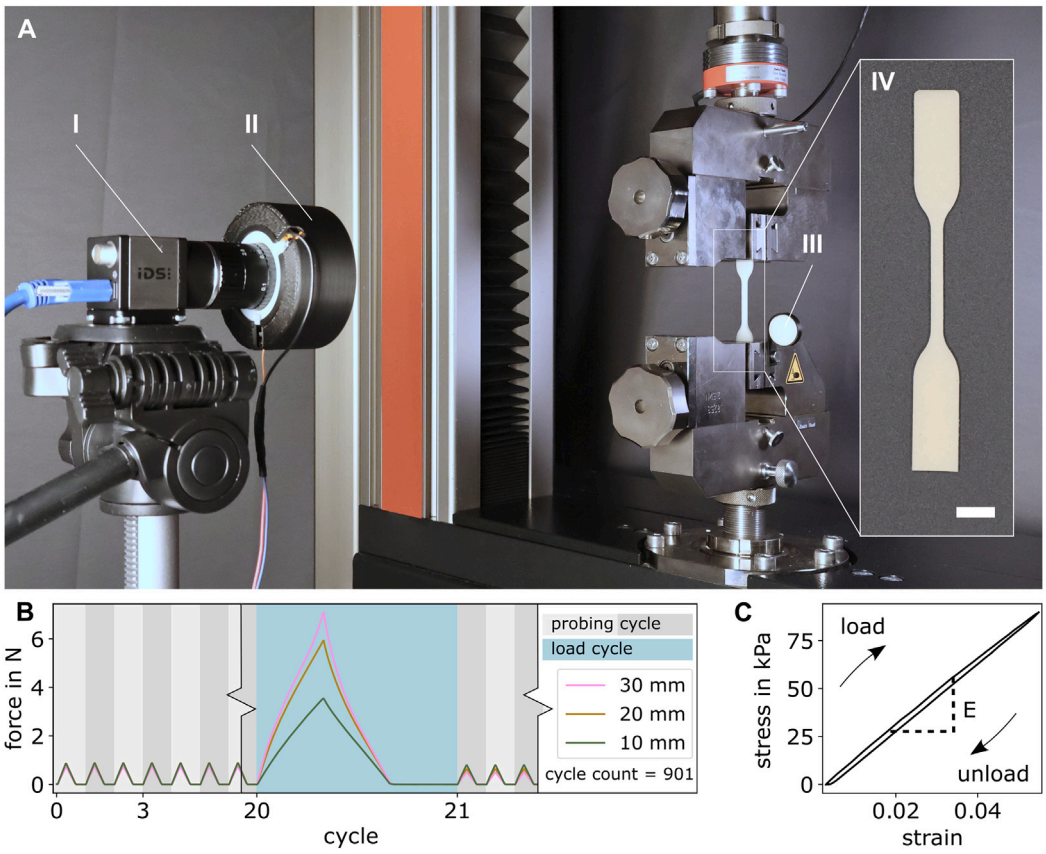


Fig. 2. (A): Test setup. I: Video camera, II: UV ring light (λ = 365–375 nm), III: Cylindrical reference specimen from the same batch as the tensile specimen, IV: Tensile specimen, scale bar = 10 mm. (B): Schematic of the testing procedure. Probing cycles are shown with light and dark gray backgrounds, while the load cycle is shown with a blue background. Each probing cycle includes a displacement-controlled load up to 2 mm, followed by unloading to zero force and a 30 s hold time. The force output in the load cycle is displayed for 30 mm, 20 mm, and 10 mm. Note that this cycle has different x-axis scaling for the three specimens. (C): Stress–strain curve of a single probing cycle, with the depiction of Young's modulus evaluation as the slope of the loading section. (For interpretation of the references to color in this figure legend, the reader is referred to the web version of this article.)

finite element simulations in COMSOL Multiphysics 6.0 (Comsol AB, Stockholm, Sweden), was applied to recalculate the strain occurring in the central gauge section, following the methodology described in [36]. Young's modulus was subsequently calculated as the slope of the linear section of the curve, as shown in Fig. 2C, and was approximately 30% higher for intact specimens as compared to pure PDMS.

To evaluate the fluorescent response due to broken microcapsules at each moment in time, the recorded video was analyzed. Pixel values were averaged over the central region of the specimen, referenced to the brightness of the non-damaged disk captured in each frame, and normalized to the initial value. This method demonstrated good correlation with spectrographic measurements (see Appendix) while offering the advantage of capturing a larger area. Similarly, Diekmann et al. demonstrated that CMOS-equipped cameras are suitable for fluorescence detection [40]. For each strain level during the loading cycle, at least three specimens were tested to ensure statistically robust conclusions.

3. Results and discussion

As-fabricated specimens exhibit a certain level of fluorescence, possibly due to initially broken capsules or damage introduced during de-molding. However, the first probing cycles confirm that no further capsule rupture occurs during testing (Fig. 3, left). Immediately after the loading cycle, the central section of the specimen begins to fluoresce, indicating the rupture of some microcapsules within the matrix and the subsequent release of their contents (Fig. 3, middle). Over time, the fluorescence intensity increases, and after 15 h, the specimen appears visibly brighter (Fig. 3, right) compared to its state immediately after the loading cycle. This observation highlights the transient nature of the self-reporting mechanism.

Fig. 4 illustrates the evolution of Young's modulus and fluorescence response following the loading cycle for specimens subjected to different strain levels. A noticeable increase in fluorescence response is observed immediately after the loading cycle, attributed to the release of contents from ruptured capsules. This increase is minimal for an applied displacement of 5 mm but becomes evident starting at 10 mm, with the magnitude of the increase growing as the displacement rises. The most pronounced fluorescence response is observed at a displacement of 30 mm (Fig. 4A). Since all other conditions were kept constant, we conclude that the increased brightness immediately after the loading cycle at higher strain levels is due to a larger number of broken capsules. While a single capsule can provide limited information about its state, the presence of multiple capsules significantly enhances the reporting capabilities. Under global deformation, such as uniaxial tension, capsules embedded in a soft matrix do not rupture simultaneously. Since directly counting the number of broken capsules is nearly impossible, indirect measures, such as changes in fluorescence or stiffness, can serve as proxies. In this case, larger changes correspond to a higher number of ruptured capsules, indicating greater achieved stresses and more significant damage. A similar approach has been shown to be effective even for relatively localized loading in microcapsule-based composites [21,34]. Simultaneously, our experiments show that for all specimens, the brightness does not remain constant but continues to

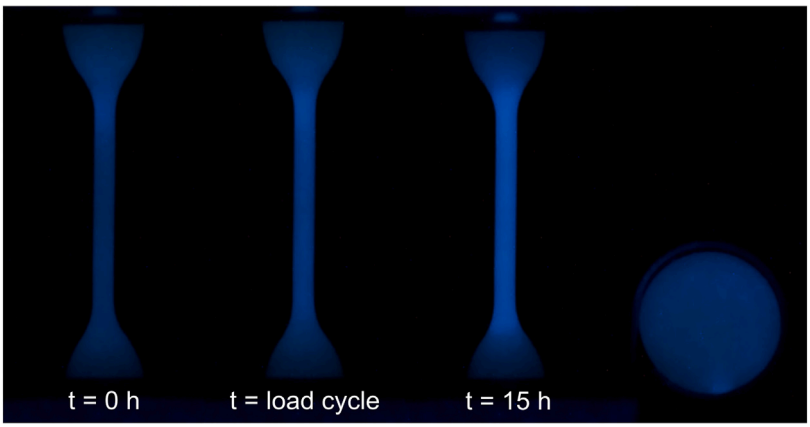


Fig. 3. Fluorescence of the tensile specimen before start of the test, immediately after loading cycle, and after 15 h (left to right). Reference cylindrical sample is shown as well. The brightness has been uniformly enhanced for visualization purposes.

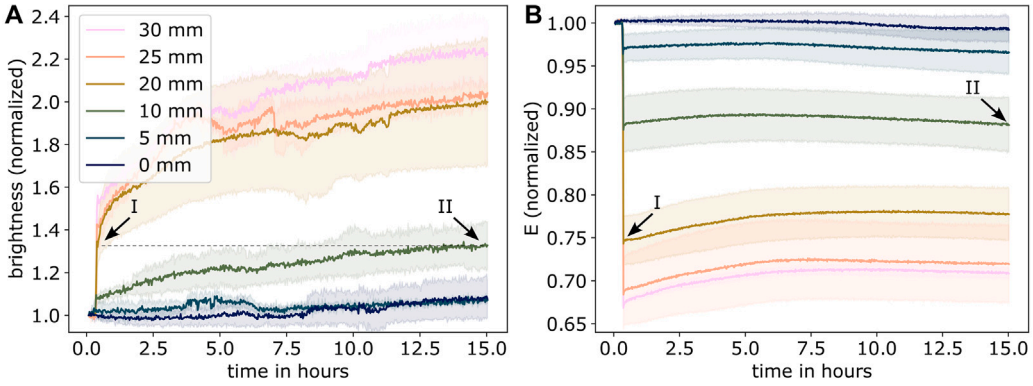


Fig. 4. Normalized brightness (A) and normalized Young's modulus (B) over time after loading to different displacements, with solid lines representing the mean and shaded areas indicating the standard deviation.

increase over the 15-hour period following the loading cycle (Fig. 4A). This effect is particularly evident for the 30 mm loading, which exhibits a 1.5-fold increase in brightness immediately after capsule rupture, with the final brightness recorded after 15 h reaching 2.2 times the initial value. The final brightness (after 15 h) follows a trend similar to the immediate post-load brightness, being higher for specimens subjected to larger displacements. Transient brightness changes after the loading cycle and capsule rupture make it difficult to correlate absolute brightness with the amount of damage unless sufficient time has passed.

As depicted in Fig. 4B, the rupture of microcapsules during loading significantly affects the composite's Young's modulus. Upon capsule breaking, we observe an immediate drop in Young's modulus of over 30% for larger displacements, such as 25 or 30 mm. At the same time, similar to the absence of immediate changes in brightness, there is no change in Young's modulus for specimens loaded only up to 2 mm, confirming that no capsules are ruptured in this case. With increasing applied displacement, the drop in Young's modulus becomes more pronounced immediately after the loading cycle. Simultaneously, a slight but gradual increase in Young's modulus is observed for specimens subjected to higher loads. This effect, though much less pronounced than the brightness changes, is primarily associated with the evaporation of solvent from the ruptured capsules and possible interaction between solvent and PDMS matrix. By combining observations of brightness and mechanical performance, we can conclude that relying solely on increase in brightness to assess damage, without considering time, can be misleading. For instance, a 30% increase in brightness might correspond to a drop in Young's modulus to 75% of its initial value if measured immediately after loading (Fig. 4, arrow I). However, if measurements are taken 15 h later, the same brightness increase may correspond to a smaller drop, down to 90% of the initial modulus (Fig. 4, arrow II).

Since both mechanical properties and fluorescence depend on the degree of damage — determined by the applied displacement during the loading cycle — it seems possible to establish a correlation by factoring in time. When the time after the loading cycle is fixed, specimens subjected to higher strains are expected to show greater changes in elastic modulus and brighter fluorescence due to the rupture of more capsules. To investigate this relationship, we plotted brightness against Young's modulus for individual specimens at three different points in time: immediately after loading (Fig. 5A), 5 hours after the start (Fig. 5B), and at the end of the observation period (Fig. 5C). Simplifying, we took the data from Fig. 4 and sliced for each selected time point.

Figs. 5A-C display a linear fit with the corresponding R^2 values, while the color represents the applied displacement during the loading cycle. Previous studies have suggested that the relationship between fluorescence and damage is generally linear, with saturation occurring when most capsules have ruptured [34]. This saturation is evident, for example, in Fig. 4B, where the properties of samples stretched to 25 mm and 30 mm are nearly identical. Our experiments further revealed that for displacements exceeding 30 mm, the PDMS matrix itself begins to fail. For the three selected times shown in Figs. 5A-C, the linear fit provides a good approximation of the dependency of Young's modulus on brightness, with R^2 values ranging from 0.9 at $t = 0$ h to 0.88 at $t = 15$ h. The data clearly shows that larger displacements result in brighter specimens and lower relative Young's modulus after capsule rupture. However, our findings also highlight an intrinsic feature of

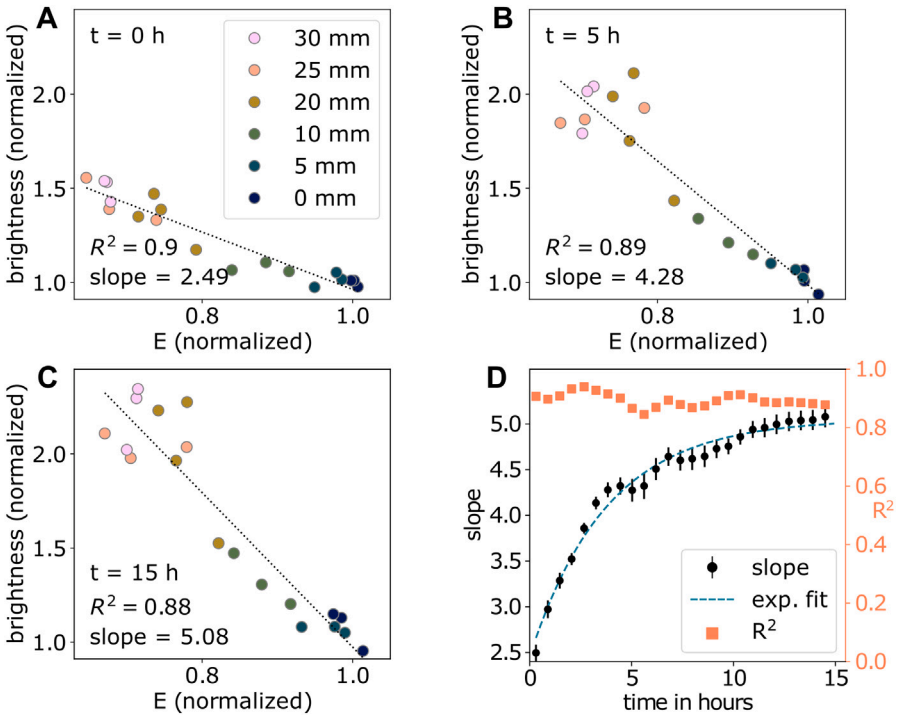


Fig. 5. Normalized brightness and normalized Young's modulus immediately after loading cycle (A), after 5 h (B), after 15 h (C). (D): Slope of the linear fit (black circles), exponential decay fit (blue line) and correlation coefficient R^2 (orange squares) over time.

self-reporting microcapsule composites: while the relationship between brightness and Young's modulus is close to linear, it evolves over time.

By performing a similar analysis and linear fitting for all available times up to 15 h, we observe that the assumption of a near-linear dependency between changes in Young's modulus and fluorescence holds true. The orange curve in Fig. 5D shows that the R^2 value for the linear fit (orange squares) remains consistently around 0.9 over time. The coefficient of proportionality m (black circles) increases over the course of the experiment, and eventually stabilizes (Fig. 5D). The coefficient m for brightness–stiffness correlation can be approximated as exponential decay function $m = m_\infty + (m_0 - m_\infty)e^{-t/\tau}$ (blue dashed line), where m_0, m_∞ and τ are fitting parameters, well-aligned with the kinetics of the evaporation process. Over time, the relationship between brightness and Young's modulus becomes more consistent as transient effects diminish and the system reaches equilibrium. This observed time-dependent evolution of the fluorescence-mechanics relationship may extend to other self-reporting composite systems, emphasizing the importance of considering temporal dynamics when interpreting damage indications.

4. Conclusions

By tracking and analyzing changes in Young's modulus and fluorescence over 15 h following the rupture of microcapsules embedded in PDMS matrix, we observed a clear correlation between fluorescence intensity and residual mechanical properties. However, the transient nature of this relationship must be considered. Fluorescence self-reporting occurs immediately after loading in the central section of the specimen, provided the applied load is sufficiently high. In this study, stretching up to 2 mm did not cause capsule rupture, while already a 5 mm displacement triggered fluorescence and a drop in Young's modulus. Both the fluorescence intensity and the decrease in Young's modulus were more pronounced for specimens subjected to higher loading, reflecting the extent of damage and the amount of ruptured capsules. While this behavior is somehow expected [13,34], the visible brightness continues to increase long after capsule rupture due to the gradual solvent evaporation process required for fluorescence. This highlights the importance of accounting for the time elapsed since the damaging event when correlating fluorescence with mechanical properties, as the transient nature of this relationship affects its accuracy. While the qualitative rule of "more damage — brighter fluorescence — lower stiffness" holds true, the exact relationship is time-dependent.

Our results demonstrate that the property–brightness relationship in the studied PDMS-microcapsule composite can be approximated as linear at any given moment, though the slope of this linear fit evolves over time and stabilizes several hours after capsule rupture. This aspect may not be critical when self-reporting is primarily used to locate damage within the matrix. In such cases, both the capsules and the load-bearing matrix material are often damaged simultaneously [14,17,21], particularly when cracks propagate through the material [9,12,13,31]. However, self-reporting can also be valuable in scenarios where capsule rupture occurs before significant matrix damage, as observed in the present study. Here, even after capsule rupture, the specimen retains its structural integrity and can withstand a slightly reduced load. Potentially, this mechanism enables the release of a self-healing agent while the matrix remains intact. Depending on the system's design, fluorescence-based self-reporting can complement self-healing in different ways. If the same capsules contain both the reporting and healing agents, fluorescence serves not only as a direct indicator of healing agent release but also as a measure of damage severity. Additionally, in the considered composites, where the elastic matrix remains intact, it becomes possible to preemptively release specific functional additives before the composite reaches total failure. In this case, fluorescence highlights the locations where specific criteria, such as reaching a critical stress level, have been met, facilitating localized changes through an additional chemical process. In general, the fluorescence of a self-reporting composite can indicate not only the extent of a specimen's property deterioration but also how close it has come to failure during previous loading. However, to achieve accurate assessments, we have shown that it is important to consider the time-dependent nature of the brightness–property relationship.

CRediT authorship contribution statement

David Schwarz: Writing – original draft, Methodology, Investigation, Formal analysis, Conceptualization. **Viacheslav Slesarenko:** Writing – review & editing, Validation, Supervision, Methodology, Funding acquisition, Conceptualization.

Declaration of Generative AI and AI-assisted technologies in the writing process

During the preparation of this work the authors used ChatGPT in order to check the grammar and slightly improve readability. After using this tool/service, the authors reviewed and edited the content as needed and take full responsibility for the content of the publication.

Declaration of competing interest

The authors declare that they have no known competing financial interests or personal relationships that could have appeared to influence the work reported in this paper.

Acknowledgments

The authors thank Dr. Celine Calvino and Dr. Claas-Hendrik Stamp for preparing the capsules and engaging in fruitful discussions. Funded by the Deutsche Forschungsgemeinschaft (DFG, German Research Foundation) under Germany's Excellence Strategy - EXC-2193/1 - 390951807. Open access funding enabled and organized by Projekt DEAL.

Appendix. Comparison of CMOS camera and spectrometer

To validate the use of the camera for fluorescence evaluation, we measured the specimens before and after the tests using a blue-wave spectrometer (StellarNet Inc., Tampa, FL, USA) and a 365 nm light source (Ocean Optics, Orlando, FL, USA). The measurements showed strong agreement, with $R^2 = 0.97$ (Fig. A.6), confirming the camera's suitability for our purposes.

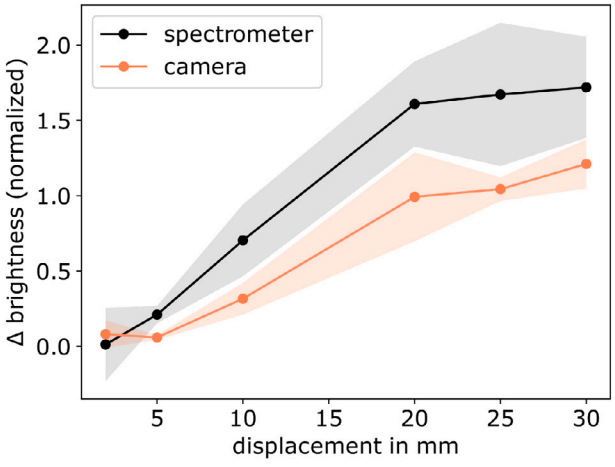


Fig. A.6. Relative change in brightness between intact specimen and after testing completion. Comparison between camera-based evaluation and spectrometer measurements, with solid points representing the mean and shaded areas indicating the standard deviation.

Data availability

Data will be made available on request.

References

[1] D.K. Rajak, D.D. Pagar, R. Kumar, C.I. Pruncu, Recent progress of reinforcement materials: a comprehensive overview of composite materials, J. Mater. Res. Technol. 8 (6) (2019) 6354–6374, http://dx.doi.org/10.1016/j.jmrt.2019.09.068.
[2] J. Pang, I. Bond, Bleeding composites—damage detection and self-repair using a biomimetic approach, Compos. Part A: Appl. Sci. Manuf. 36 (2) (2005) 183–188, http://dx.doi.org/10.1016/s1359-835x(04)00166-6.
[3] J.W. Pang, I.P. Bond, A hollow fibre reinforced polymer composite encompassing self-healing and enhanced damage visibility, Compos. Sci. Technol. 65 (11–12) (2005) 1791–1799, http://dx.doi.org/10.1016/j.compscitech.2005.03.008.
[4] H. Chang, Z. Guo, C. Chen, H. Zhang, Z. Li, X. Wang, J. Liu, Mechanical properties, durability and self-healing performance of mortar containing double-layers capsules, Mater. Today Commun. 38 (2024) 107880, http://dx.doi.org/10.1016/j.mtcomm.2023.107880.
[5] M.M. Caruso, B.J. Blaiszik, S.R. White, N.R. Sottos, J.S. Moore, Full recovery of fracture toughness using a nontoxic solvent-based self-healing system, Adv. Funct. Mater. 18 (13) (2008) 1898–1904, http://dx.doi.org/10.1002/adfm.200800300.
[6] C.E. Diesendruck, N.R. Sottos, J.S. Moore, S.R. White, Biomimetic self-healing, Angew. Chem. Int. Ed. 54 (36) (2015) 10428–10447, http://dx.doi.org/10.1002/anie.201500484.
[7] S.A. McDonald, S.B. Coban, N.R. Sottos, P.J. Withers, Tracking capsule activation and crack healing in a microcapsule-based self-healing polymer, Sci. Rep. 9 (1) (2019) http://dx.doi.org/10.1038/s41598-019-54242-7.
[8] H. Yuan, H. Chen, M.I. Khan, Z. Lv, J. Lin, Analytical models for crack-hitting probability and crack-healing efficiency by linear capsules in a material with parallelogram crack network, Mater. Today Commun. 41 (2024) 111048, http://dx.doi.org/10.1016/j.mtcomm.2024.111048.
[9] S.R. White, N.R. Sottos, P.H. Geubelle, J.S. Moore, M.R. Kessler, S.R. Sriram, E.N. Brown, S. Viswanathan, Autonomic healing of polymer composites, Nature 409 (6822) (2001) 794–797, http://dx.doi.org/10.1038/35057232.
[10] E.N. Brown, N.R. Sottos, S.R. White, Fracture testing of a self-healing polymer composite, Exp. Mech. 42 (4) (2002) 372–379, http://dx.doi.org/10.1007/bf02412141.
[11] D.Y. Zhu, M.Z. Rong, M.Q. Zhang, Self-healing polymeric materials based on microencapsulated healing agents: From design to preparation, Prog. Polym. Sci. 49–50 (2015) 175–220, http://dx.doi.org/10.1016/j.progpolymsci.2015.07.002.
[12] M. Kosarli, D.G. Bekas, K. Tsirka, D. Baltzis, D.T. Vaimakis-Tsogkas, S. Orfanidis, G. Papavassiliou, A.S. Paipetis, Microcapsule-based self-healing materials: Healing efficiency and toughness reduction vs. capsule size, Compos. Part B: Eng. 171 (2019) 78–86, http://dx.doi.org/10.1016/j.compositesb.2019.04.030.
[13] V.K. Mohonee, K.L. Goh, L. Mishnaevsky, P. Pasbakhsh, Capsule based self-healing composites: New insights on mechanical behaviour based on finite element analysis, Comput. Mater. Sci. 192 (2021) 110203, http://dx.doi.org/10.1016/j.commatsci.2020.110203.
[14] Y. Wang, W. Tan, X. Luo, X. Rao, Y. Wang, J. Wang, W. Suphamitmongkol, T. Chowwanonthapunya, L. Ma, D. Zhang, A novel self-healing coating with mechanically-triggered self-reporting properties: Color and fluorescence dual damage indications, Prog. Org. Coatings 187 (2024) 108147, http://dx.doi.org/10.1016/j.porgcoat.2023.108147.
[15] V.H. de Souza Rodrigues, A. Estêvão Carrara, S.S. Rossi, L. Mattos Silva, R. de Cássia Lazzarini Dutra, J.C.N. Dutra, Synthesis, characterization and qualitative assessment of self-healing capacity of PU microcapsules containing TDI and IPDI as a core agent, Mater. Today Commun. 21 (2019) 100698, http://dx.doi.org/10.1016/j.mtcomm.2019.100698.
[16] Z. Yin, J. Guo, J. Qiao, X. Chen, Improved self-healing properties and crack growth resistance of polydimethylsiloxane elastomers with dual-capsule room-temperature healing systems, Colloid Polym. Sci. 298 (1) (2019) 67–77, http://dx.doi.org/10.1007/s00396-019-04587-2.
[17] E.T.A. van den Dungen, B. Loos, B. Klumperman, Use of a profluorophore for visualization of the rupture of capsules in self-healing coatings, Macromol. Rapid Commun. 31 (7) (2010) 625–628, http://dx.doi.org/10.1002/marc.200900728.
[18] S.A. Odom, A.C. Jackson, A.M. Prokup, S. Chayanupatkul, N.R. Sottos, S.R. White, J.S. Moore, Visual indication of mechanical damage using core–shell microcapsules, ACS Appl. Mater. Interfaces 3 (12) (2011) 4547–4551, http://dx.doi.org/10.1021/am201048a.
[19] S. Vidinejevs, O. Strekalova, A. Aniskevich, S. Gaidukov, Development of a composite with an inherent function of visualization of a mechanical action, Mech. Compos. Mater. 49 (1) (2013) 77–84, http://dx.doi.org/10.1007/s11029-013-9323-9.
[20] J.F. Patrick, M.J. Robb, N.R. Sottos, J.S. Moore, S.R. White, Polymers with autonomous life-cycle control, Nature 540 (7633) (2016) 363–370, http://dx.doi.org/10.1038/nature21002.
[21] M.J. Robb, W. Li, R.C.R. Gergely, C.C. Matthews, S.R. White, N.R. Sottos, J.S. Moore, A robust damage-reporting strategy for polymeric materials enabled by aggregation-induced emission, ACS Central Sci. 2 (9) (2016) 598–603, http://dx.doi.org/10.1021/acscentsci.6b00198.
[22] Y. Yoo, C. Martinez, J.P. Youngblood, Sustained dye release using Poly(urea–urethane)/cellulose nanocrystal composite microcapsules, Langmuir 33 (6) (2017) 1521–1532, http://dx.doi.org/10.1021/acs.langmuir.6b04628.

[23] R. Rajamanickam, K. Kwon, G. Tae, Soft and elastic hollow microcapsules embedded silicone elastomer films with enhanced water uptake and permeability for mechanical stimuli responsive drug delivery applications, Mater. Sci. Eng.: C 111 (2020) 110789, http://dx.doi.org/10.1016/j.msec.2020.110789.

[24] C. Calvino, E. Henriet, L.F. Muff, S. Schrettl, C. Weder, Mechanochromic polymers based on microencapsulated solvatochromic dyes, Macromol. Rapid Commun. 41 (7) (2020) http://dx.doi.org/10.1002/marc.201900654.

[25] M. Hu, Z. Ma, M. Kim, D. Kim, S. Ye, S. Pané, Y. Bao, R.W. Style, L. Isa, Self-reporting multiple microscopic stresses through tunable microcapsule arrays, Adv. Mater. (2024) http://dx.doi.org/10.1002/adma.202410945.

[26] P. Scholle, M. Sinapius, Influence of the electrical anisotropy of unidirectional carbon fiber reinforced plastics on their self strain sensing properties, Compos. Part C: Open Access 8 (2022) 100256, http://dx.doi.org/10.1016/j.jcomc.2022.100256.

[27] H. Ono, Micromechanical analysis for effective elastic moduli and thermal expansion coefficient of composite materials containing ellipsoidal fillers oriented randomly, Compos. Part C: Open Access 14 (2024) 100482, http://dx.doi.org/10.1016/j.jcomc.2024.100482.

[28] A. Teimouri, R. Barbaz Isfahani, S. Saber-Samandari, M. Salehi, Experimental and numerical investigation on the effect of core-shell microcapsule sizes on mechanical properties of microcapsule-based polymers, J. Compos. Mater. 56 (18) (2022) 2879–2894, http://dx.doi.org/10.1177/00219983221107831.

[29] W. Meier, Polymer nanocapsules, Chem. Soc. Rev. 29 (5) (2000) 295–303, http://dx.doi.org/10.1039/a809106d.

[30] M. Hu, S. Peil, Y. Xing, D. Döhler, L.C. da Silva, W.H. Binder, M. Kappl, M.B. Bannwarth, Monitoring crack appearance and healing in coatings with damage self-reporting nanocapsules, Mater. Horizons 5 (1) (2018) 51–58, http://dx.doi.org/10.1039/c7mh00676d.

[31] M. Keller, S. White, N. Sottos, A self-healing Poly(Dimethyl Siloxane) elastomer, Adv. Funct. Mater. 17 (14) (2007) 2399–2404, http://dx.doi.org/10.1002/adfm.200700086.

[32] A. Tabatabaeian, S. Liu, P. Harrison, E. Schlangen, M. Fotouhi, A review on self-reporting mechanochromic composites: An emerging technology for structural health monitoring, Compos. Part A: Appl. Sci. Manuf. 163 (2022) 107236, http://dx.doi.org/10.1016/j.compositesa.2022.107236.

[33] C. Calvino, A. Guha, C. Weder, S. Schrettl, Self-calibrating mechanochromic fluorescent polymers based on encapsulated excimer-forming dyes, Adv. Mater. 30 (19) (2018) 1704603, http://dx.doi.org/10.1002/adma.201704603.

[34] C. Calvino, C. Weder, Microcapsule-containing self-reporting polymers, Small 14 (46) (2018) 1802489, http://dx.doi.org/10.1002/smll.201802489.

[35] C. Calvino, Polymer-based mechanochromic composite material using encapsulated systems, Macromol. Rapid Commun. 42 (1) (2020) 2000549, http://dx.doi.org/10.1002/marc.202000549.

[36] F. Schneider, T. Fellner, J. Wilde, U. Wallrabe, Mechanical properties of silicones for MEMS, J. Micromech. Microeng. 18 (6) (2008) 065008, http://dx.doi.org/10.1088/0960-1317/18/6/065008.

[37] M.M. Caruso, B.J. Blaiszik, H. Jin, S.R. Schelkopf, D.S. Stradley, N.R. Sottos, S.R. White, J.S. Moore, Robust, double-walled microcapsules for self-healing polymeric materials, ACS Appl. Mater. Interfaces 2 (4) (2010) 1195–1199, http://dx.doi.org/10.1021/am100084k.

[38] M.W. Keller, N.R. Sottos, Mechanical properties of microcapsules used in a self-healing polymer, Exp. Mech. 46 (6) (2006) 725–733, http://dx.doi.org/10.1007/s11340-006-9659-3.

[39] C.-H. Stamp, J. Stumpp, C. Calvino, Adhesives with debonding-on-demand capability: Leveraging responsive microcapsules for mechanically-induced debonding, Adv. Mater. (2025) e2414308, http://dx.doi.org/10.1002/adma.202414308.

[40] R. Diekmann, K. Till, M. Müller, M. Simonis, M. Schüttpelz, T. Huser, Characterization of an industry-grade CMOS camera well suited for single molecule localization microscopy – high performance super-resolution at low cost, Sci. Rep. 7 (1) (2017) http://dx.doi.org/10.1038/s41598-017-14762-6.